



α -ZrP/Uracil/Cu²⁺ nanoparticles as an efficient catalyst in the Morita-Baylis-Hillman reaction

Abdol R. Hajipour | Saedeh Zakery

Pharmaceutical Research Laboratory,
Department of Chemistry, Isfahan
University of Technology, Isfahan
84156-83111, Iran

Correspondence

Abdol R. Hajipour, Pharmaceutical
Research Laboratory, Department of
Chemistry, Isfahan University of
Technology, 84156-83111, Isfahan, Iran.
Email: haji@cc.iut.ac.ir

A facile synthesis of uracil-Cu²⁺ nanoparticles immobilized on *alpha*-zirconium hydrogen phosphate (α -ZrP), abbreviated as α -ZrP/Uracil/Cu²⁺, was presented. This compound was synthesized by the thermal method and used as a reusable catalyst for the Morita-Baylis-Hillman reaction without any additives. First, (3-iodopropyl) trimethoxysilane as a linker is reacted with α -ZrP support to give the α -ZrP/IPTMOS. Addition of uracil and then the addition of copper (II) acetate to α -ZrP/IPTMOS results in the production of selected catalyst. The Morita-Baylis-Hillman reaction catalyzed by α -ZrP/Uracil/Cu²⁺ demonstrated high product yield, short reaction time and a straightforward work-up. The catalyst with enough outside surface was easily recovered using centrifugation and reused five times without a significant reduction in its activity.

KEYWORDS

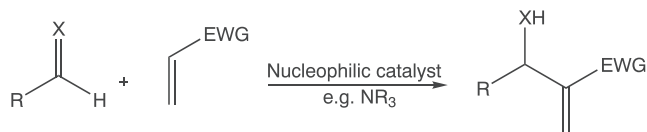
Morita-Baylis-Hillman reaction, nanocatalyst, uracil, zirconium hydrogen phosphate support

1 | INTRODUCTION

The Morita Baylis-Hillman reaction (MBH) has been used in the various synthetic methodologies for making the carbon-carbon bonds.^[1-4] It includes the α -carbon bonding in an activated vinyl system to electrophilic carbon (sp^2) in carbonyl compounds, catalyzed by the nucleophilic catalyst such as tertiary amines and phosphines (Scheme 1).^[5,6] Multifunctional products of MBH reaction, allylic alcohols, are used as the building block for the synthesis of natural compounds and drugs.^[7,8] Most of these compounds have biological properties.^[8,9] Also, these products can play the role of starting material or intermediate on total synthesis in organic chemistry.^[6,10,11]

A brief survey in the old published articles displays that, the MBH reactions suffered from a low reaction rate.^[12] Therefore, the attention of scientists has been drawn to the design of different methods to increase the MBH reaction rate and yield. Based on previous researches, the use of high pressures,^[4,5] organocatalysis,^[12] type of ligands^[13] and the activated

vinyl system and electrophile^[14] can improve the reaction conditions. Many additives were also used as co-catalyst to accelerate this reaction, such as La (OTf)₃,^[15] lithium perchlorate,^[16] urea^[17] and Brønsted acid.^[18] One of the most challenges in the MBH reaction is to design a suitable and renewable catalyst to improve the reaction rate. The focus and main goal of this research are to the preparation of a new nanocatalyst without any additives to reduce the MBH reaction time and increase its efficiency. {Uracil-Cu}-propyltrimethoxysilane immobilized on *alpha*-zirconium hydrogen phosphate used in this reaction. ZrP is an important class of crystalline layered multi-functional materials with well-ordered structure^[19] which has been synthesized by various methods.^[20,21] In the layered structure of this material, the Zr (IV) ions are located on the top and bottom of each layer. By connecting each Zr⁴⁺ cations to the three oxygen atoms of the phosphate groups, the hydroxyl group of the phosphate groups points to the interlayer space and interacts chemically with water molecules located between the layers. In the presence of these hydrogens, ZrP will be a Brønsted acid.^[21] Due to the presence of



R = alkyl, aryl, heteroaryl
X = O, NCO₂R, NTs, NSO₂Ph.
EWG = COR, CHO, CN, CO₂R

SCHEME 1 The MBH reaction^[4]

the hooked P-OH groups on the surface of ZrP, it will be used as a suitable support for immobilization various materials such as drugs, enzymes (enzyme-controlled drug delivery) and catalysts.^[20,22,23] Immobilized catalysts can be prepared by a linker with long alkyl chain^[24] to connect a homogeneous catalyst to a solid support. Hence, this material has been used as a heterogeneous solid acid catalyst in many organic synthesis reactions.^[25,26] The layered structure of these compounds results in the interlayer intercalation of many compounds into ZrP, especially type of drugs.^[27,28] Previous researches have shown the potential for conversion of ZrP to nanoparticles,^[29–31] nanoplates^[21,32] and nanocomposites.^[33,34] There are some new polymers such as polyvinylpyrrolidone polymers (PVP) based precursor methods to prepare nanoparticles.^[34–36] These polymers, as the dispersing agents, can play an important role in the production of nano-sized particles.^[37,38] The best type of crystalline ZrP is α -phase. Its composition has been defined as Zr (HPO₄)₂·H₂O.^[39–41] In previous studies, the interlayer spacing of 7.4–7.6 Å for the planes of this compound is revealed by X-ray powder diffraction (XRPD).^[31,42,43]

According to the latest literature, there is no report to use ZrP-based nanocatalysts for MBH reaction. Accordingly, in continuation of our research, to design an efficient catalyst, we have investigated MBH reaction over α -ZrP/Uracil/Cu²⁺ nanoparticles under different conditions. The reaction conditions such as solvent, the amount of catalyst and temperature were tested in details.

2 | EXPERIMENTAL

All chemical reagents were purchased from Aldrich and Merck Chemical Company and were used without further purification. X-ray diffraction (XRD) powder patterns were obtained using a Philips X'pert X-ray diffractometer, with Cu K α radiation (40 kV, 30 mA). The Brunauer–Emmett–

Teller (BET) method on a Quantachrome ChemBET 3000 instrument was used for N₂ adsorption–desorption isotherm. TEM (Philips CM10 microscope) and SEM (MIRA3 TESCAN) were used to characterize the catalyst.

TPD-NH₃ with a Quantachrome ChemBET 3000 was used for the measuring the total acidity of α -ZrP. FT-IR spectroscopy (JASCO FT-IR 680-Plus spectrophotometer) was employed for characterization of the α -ZrP/Uracil/Cu²⁺ catalyst. Also Inductive coupled plasma Perkin Elmer Optima 7300 DV was used. ¹H NMR spectra was recorded with a Bruker (300 MHz) Avance DRX in the pure DMSO-*d*₆ solvent with tetramethylsilane as internal standard. TGA of the α -ZrP/Uracil/Cu²⁺ catalyst was conducted using a lab-made TGA instrument.

2.1 | α -ZrP preparation

A 20% solution of Polyvinylpyrrolidone (PVP) (Mw = 40,000) was prepared by dissolving the polymer in deionized hot water under stirring at 90 °C. Then the pH value was adjusted by adding HCl to below 2. Zirconyl chloride octahydrate (ZrOCl₂·8H₂O) was used as a zirconium source in this experiment. 30 ml of the 1 M solution of ZrOCl₂·8H₂O was added dropwise to the PVP solution and heated at 80 °C for 12 hr using magnetic stirrer. By adding a drop by drop of 10 ml concentrated phosphoric acid to the previous homogeneous solution, zirconium phosphate begins to produce. After 3 hours, the stirring was stopped and the mixture was kept at ambient temperature for 10 hr. After this step, the resulting precipitate was filtered and washed with ethanol and distilled water. The obtained white powder was finally dried in an oven at 70 °C overnight. In order to decompose the polymer chains, white powder was calcined at 600 °C for 3 hours. The final product is α -ZrP nanoparticles.

2.2 | α -ZrP/Uracil/Cu²⁺ preparation

2 g of α -ZrP in 40 ml of dry toluene was dispersed for 1 hour, then 3.5 mmol of IPTMOS was added to the previous mixture and refluxed to 100 °C for 48 hr. After that time, the resulting precipitate was filtrated, washed with dichloromethane and dried at room temperature. In a round-bottomed flask, 2 g of dried powder, 15 ml of DMF, 2 mmol of uracil (0.22 g) and 3 mmol of cesium carbonate (0.96 g) were added. This mixture was heated at 80 °C for 24 hours under argon. After this step, the white precipitate was collected and washed with ethanol several times. The powder drying was carried out in a vacuum oven at 50 °C overnight. In order to add a catalyst metal section, 1 g of the modified support is dispersed in 30 ml of ethanol. Then 0.2 g of copper (II) acetate monohydrate was dissolved in 10 ml of ethanol and was added to the dispersed mixture over two hours. The resulting mixture stirred for 1 hr at room temperature and then was sonicated for 15 min. The precipitate was

collected and washed with acetone and ethanol. After drying in a vacuum oven at 50 °C, the desired catalyst was obtained as a blue solid.

2.3 | MBH reaction catalyzed by α -ZrP/Uracil/Cu²⁺

To a solution of methyl acrylate (1.2 mmol) and aldehyde (1 mmol) in 3 ml DMF, 20 mg of catalyst was added and stirred at room temperature for 12 hours. The progress of the reaction was monitored by TLC. After consumption of aldehyde, the reaction mixture was cooled and then the catalyst was separated by centrifugation. After extraction the remaining solution with ethyl acetate (3 × 10 ml), the organic phase was dried by CaCl₂. The product was purified by column chromatography (*n*-hexane/ethyl acetate, 3:1). The physical and spectroscopic data for selected compounds are listed below and the original spectra for these molecules could be found in the supporting information file.

A. Methyl 2-(hydroxy (pyridin-3-yl)methyl)acrylate

White solid, **mp**: 170–172 °C; ¹H NMR (300 MHz, DMSO-*d*₆): δ 3.71 (s, 3H), 4.85 (s, 1H), 5.61 (s, 1H), 6.01 (s, 1H), 6.40 (s, 1H), 7.27 (dd, *J* = 12 Hz, 1H), 7.74 (d, *J* = 6.0 Hz, 1H), 8.45 (d, *J* = 15.0 Hz, 2H).

B. Methyl 2-(hydroxy (naphthalen-2-yl)methyl)acrylate

White solid, **mp**: 132–134 °C; ¹H NMR (300 MHz, DMSO-*d*₆): δ 3.23 (s, 1H), 3.60 (s, 3H), 5.63 (s, 1H), 5.79 (s, 1H), 6.29 (s, 1H), 7.38 (m, 3H), 7.72 (m, 4H).

C. Methyl 4-(1-hydroxy-2-(methoxycarbonyl)allyl)benzoate

White solid, **mp**: 140–142 °C; ¹H NMR (300 MHz, DMSO-*d*₆): δ 3.68 (s, 3H), 3.87 (s, 4H), 5.57 (s, 1H), 5.88 (s, 1H), 6.33 (s, 1H), 7.43 (d, *J* = 12 Hz, 2H), 7.96 (d, *J* = 12 Hz, 2H).

D. Methyl 2-(hydroxy (3-methoxyphenyl)methyl)acrylate

Yellow solid, **mp**: 151–153 °C; ¹H NMR (300 MHz, DMSO-*d*₆): δ 3.19 (s, 1H), 3.63 (s, 3H), 3.73 (s, 3H), 5.44 (s, 1H), 5.76 (s, 1H), 6.25 (s, 1H), 6.73 (dd, *J* = 9 Hz, 1H), 6.85 (m, 2H), 7.17 (m, 1H).

E. Methyl 2-(hydroxy (3-nitrophenyl)methyl)acrylate

White solid, **mp**: 133–135 °C; δ 3.63 (s, 3H), 5.60 (s, 1H), 6.10 (s, 1H), 6.14 (s, 1H), 6.29 (s, 1H), 7.63 (t, *J* = 15 Hz, 1H), 7.78 (d, *J* = 9 Hz, 1H), 8.14 (m, 2H).

F. 2-(hydroxy (phenyl)methyl)cyclopent-2-en-1-one

Brown solid, **mp**: 162–163 °C; ¹H NMR (300 MHz, DMSO-*d*₆): δ 2.30 (t, *J* = 8 Hz, 2H), 2.56 (m, 2H), 3.64 (s, 1H), 5.32 (s, 1H), 5.64 (t, *J* = 8 Hz, 1H), 7.31 (m, 5H).

G. 2-(hydroxy (4-methoxyphenyl)methyl)acrylamide

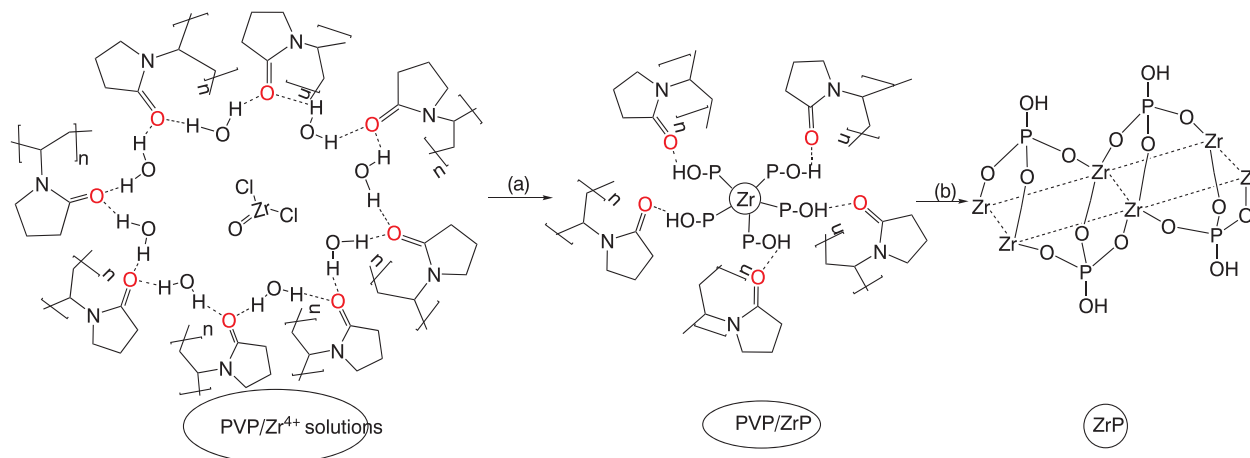
Brown solid, **mp**: 148–149 °C; ¹H NMR (300 MHz, DMSO-*d*₆): δ 2.72 (s, 1H), 3.74 (s, 3H), 4.49 (s, 1H), 4.91 (s, 1H), 5.48 (s, 1H), 6.35 (dd, *J* = 10 Hz, 2H), 7.25 (dd, *J* = 10 Hz, 2H), 7.70 (t, *J* = 2 Hz, 2H).

3 | RESULTS AND DISCUSSION

3.1 | Support material

Initially, α -ZrP nanoparticles as support with an average particle size of 65 nm have been prepared. By adding phosphate ions to the PVP/Zr⁴⁺ solutions, a white solid product, namely α -ZrP, was quickly formed. Polymeric chains of PVP, like a capsule around Zr (IV) ions, prevent them from sticking together. Also, this organic matrix can act as the dispersing agent of particles.^[26] H-bond interactions between the polar sites of polymer chains, water molecules around the Zr (IV) ions and the P-OH groups of α -ZrP have an effective role in the better distribution of α -ZrP particles. After calcination of PVP/ZrP at 600 °C for 3 hr and decomposition of the polymer chains, pure α -ZrP nanoparticles were obtained. A brief synthetic route for the preparation of these nanoparticles is depicted in Scheme 2. FT-IR Spectroscopy was used to confirm the structure of α -ZrP (Figure 1). As can be observed, there are several main absorption bands in 3435, 1630, 1070 and 605 cm⁻¹. The broad band at 3435 cm⁻¹ and the sharp band at 1630 cm⁻¹ ascribed to the asymmetric O-H stretching and bending of the O-H bonds, respectively. The strong sharp and broad band at 1070 cm⁻¹ corresponded to the P-O symmetrical stretching vibration of PO₄³⁻ groups. Also, Zr-O bond stretching vibrations located at 605 cm⁻¹ (Figure 1).^[44,45]

The nitrogen adsorption-desorption isotherm (the BET method) was used to investigate the α -ZrP specific surface area. Before each analysis, in order to remove any adsorbent on the surface, the sample was degassed at 400 °C for 3 hr. Three adsorption stages are recognizable from the isotherm. The first stage is in P/Po < 0.38, the next stage is in 0.38 < P/Po < 0.86 and the third stage in higher partial pressure (P/Po > 0.86). The total surface area of 120.1 m² g⁻¹ was obtained. As shown in Figure 2,



SCHEME 2 Preparation of α -ZrP nanoparticles: (a) 12 M H₃PO₄, H₂O, reflux, 6 h; (b) Calcination at 600 °C, 3 hr

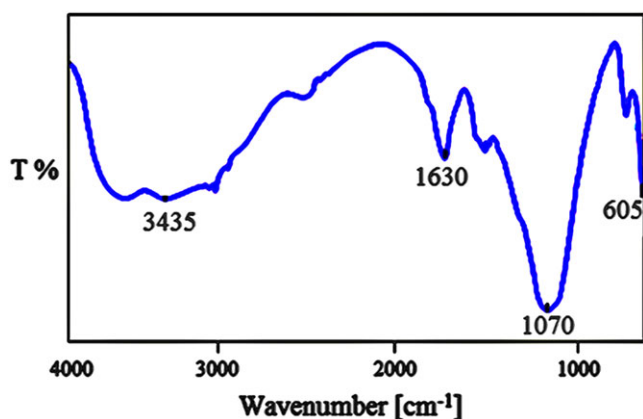


FIGURE 1 FT-IR spectra of α -ZrP

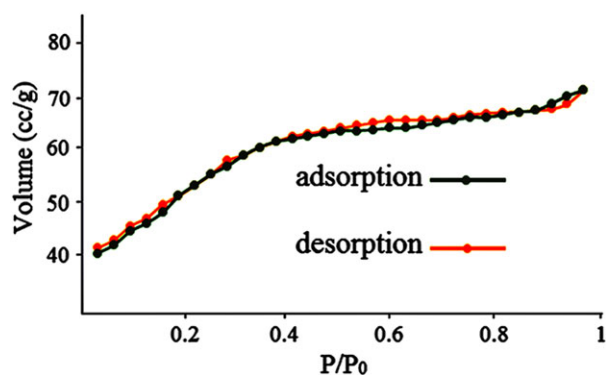


FIGURE 2 Nitrogen adsorption-desorption isotherms of α -ZrP

increase in absorption at a higher relative pressure (P/P₀) indicates a large surface area in the α -ZrP structure.^[26]

Thermodesorption curves for ammonia (NH₃-TPD) has been used to measure the surface acidity of the α -ZrP (Figure 3). The absorption of ammonia by α -ZrP is carried out at a temperature between 150 to 650 °C, which corresponds to the number of medium and the strong acidic sites. The desorption peak below 250 °C demonstrates

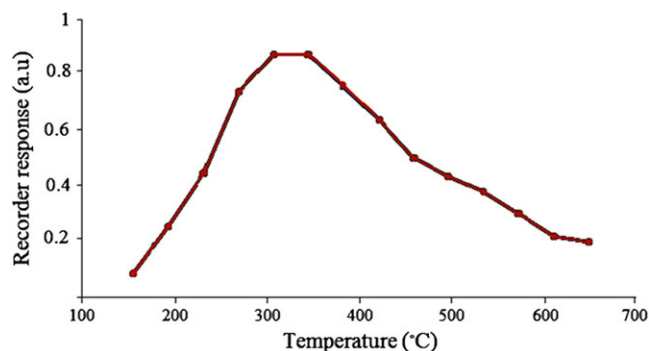
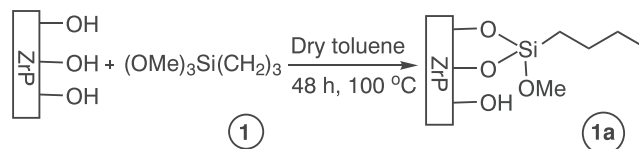


FIGURE 3 TPD ammonia curve over α -ZrP

the weak acidic sites. The NH₃ desorption temperature peak at 250-450 °C belongs to the moderate acidic sites. Finally, the desorption peak at 450-650 °C shows the strong acidic sites on the surface of α -ZrP.^[46-48] This indicates that the acidity of the α -ZrP is in the moderate range (1.65 mmol NH₃ g⁻¹) which is attributed to the presence of P-OH groups on the surface of α -ZrP.

3.2 | Surface modification of α -ZrP with immobilization of the linker

Linker **1** (IPTMOS) has been immobilized on the α -ZrP surface to form **1a** using the reported method for immobilization on oxide supports (Scheme 3).^[49-53] The compound **1a** was prepared by heating a mixture of **1** and α -ZrP in dry toluene to 100 °C for 48 hr. The



SCHEME 3 Surface modification of α -ZrP

prepared material **1a** is separated from the reaction media by filtration and washed with dry toluene. Finally, after drying, a white powder is obtained. This material was analyzed by XRD, FT-IR and ICP-OES. The powder XRD patterns of the α -ZrP and **1a** are shown in Figure 4a and b. Similar reflections are observed in the X-ray diffractogram of two compounds in the 2θ range of $5\text{--}40^\circ$. It is observed that the peaks are broadened after immobilization. According to the peak at $2\theta = 12^\circ$ the basal spacing of the (002) plane in α -ZrP is 7.5 \AA .^[31,54] Above all, **1a** is not entered between the α -ZrP layers during the immobilization process because the same interlayer spacing is exactly observed in **1a** (Figure 4b).

The FT-IR spectra of **1** and **1a** are shown in Figure 5a and b. The Specific bands of **1** appearing at 2943 and 2841 cm^{-1} correspond to the sp^3 C-H stretching of methylene groups. The observation of this absorption band at 2924 and 2854 cm^{-1} and also the main characteristic bands of α -ZrP at 3422 , 1637 , 1061 and 607 cm^{-1} in the FT-IR spectra of **1a** is a proof of immobilization of the linker **1**.

ICP-OES analysis was used to determine the Zr and Si contents of the **1a**. These analytical results are Zr (11.20), Si (1.46), P (19.1) and O (61.23) wt. %.

3.3 | Immobilization of the catalyst

The immobilized catalyst **1b** has been obtained from **1a** by iodine exchange with uracil and addition of Cu (OAc)₂ at 110°C (Scheme 4).

The important point is uracil does not intercalate between the α -ZrP layers (Figure 6). Also, copper has not been replaced by the hydrogen atoms of P-OH groups.^[55] This is investigated by the XRD pattern of **1b**, which indicates that the peak corresponding to the

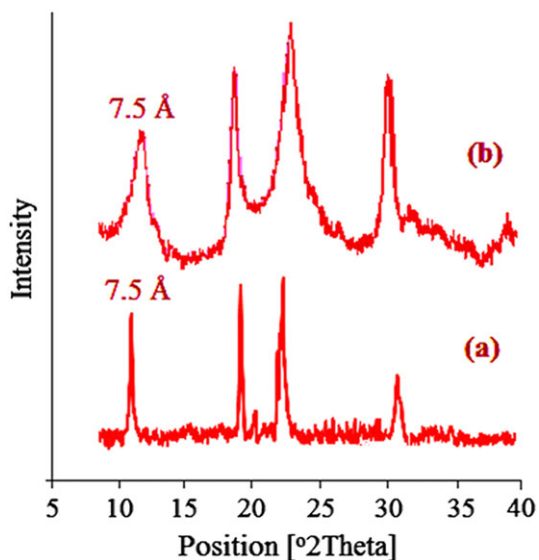


FIGURE 4 XRD pattern of α -ZrP (a) and **1a** (b)

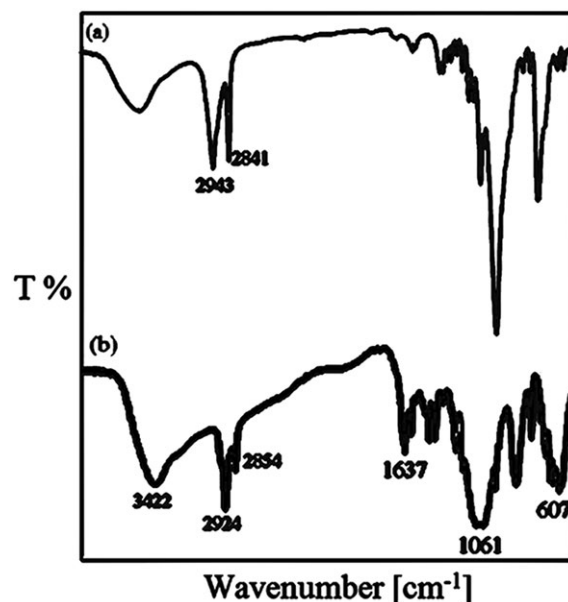
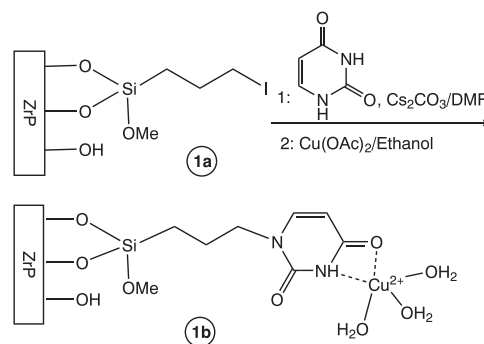


FIGURE 5 FT-IR spectra of **1** (a) and **1a** (b)



SCHEME 4 Formation of the immobilized catalyst **1b**

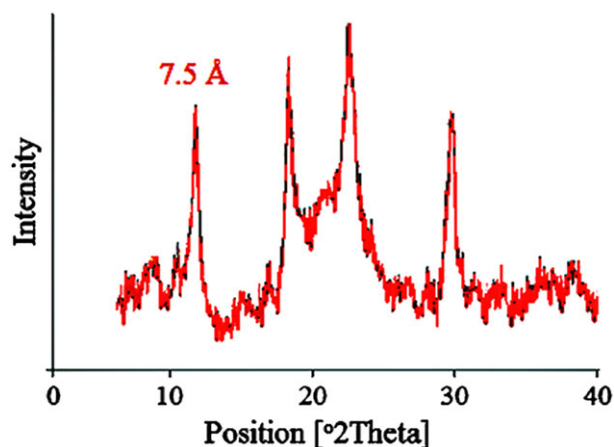


FIGURE 6 XRD pattern of **1b**

layer spacing of 7.5 \AA in analogy to the display in Figure 4.

In the FT-IR spectrum of uracil, the main characteristic vibrational band appears in 3112 , 1710 , 1630 , 1507 ,

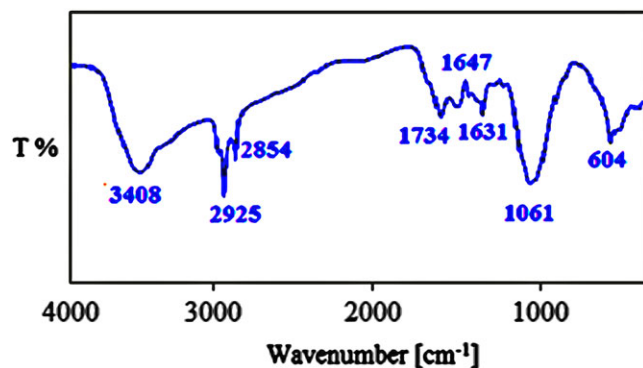


FIGURE 7 FT-IR spectra of 1b

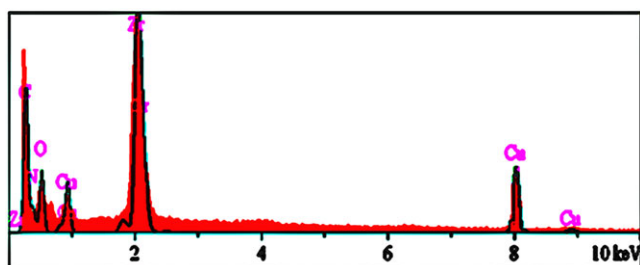


FIGURE 8 EDS spectrum of 1b as catalyst

1451, 1414 and 1387 cm^{-1} .^[56] The observation of the main absorption bands of **1a** and uracil with variations in the frequency in the FT-IR spectrum of **1b** is a reason for iodine substitution with uracil (Figure 7).^[57–59]

The presence of C, O, N, Zr and Cu in the structure of **1b** as the catalyst were confirmed by EDS analysis (Figure 8). The CHNS analysis also showed the exact contents of these elements; C: 15.09%, H: 1.53% and N: 4.60%.

The quantitative of the Zr, Si and Cu contents, as determined by ICP-OES were obtained to be 10.67, 0.95 and 1.07%, respectively.

SEM microscopy was used for nanocatalyst surface analysis. As shown in Figure 9a, the SEM micrograph a series of uniform particles with a smooth surface and a large dispersion. The TEM image confirms good monodispersity of nanoparticles (Figure 9b). Using the Dynamic light scattering (DLS) method, the average particle size of the catalyst was calculated to be 62 nm (Figure 9c).

Thermogravimetric analysis (TGA) was used to measure the thermal stability of catalyst (Figure 10). As shown in the curve, approximately 7% of the weight was lost from room temperature to 120 °C is related to the loss

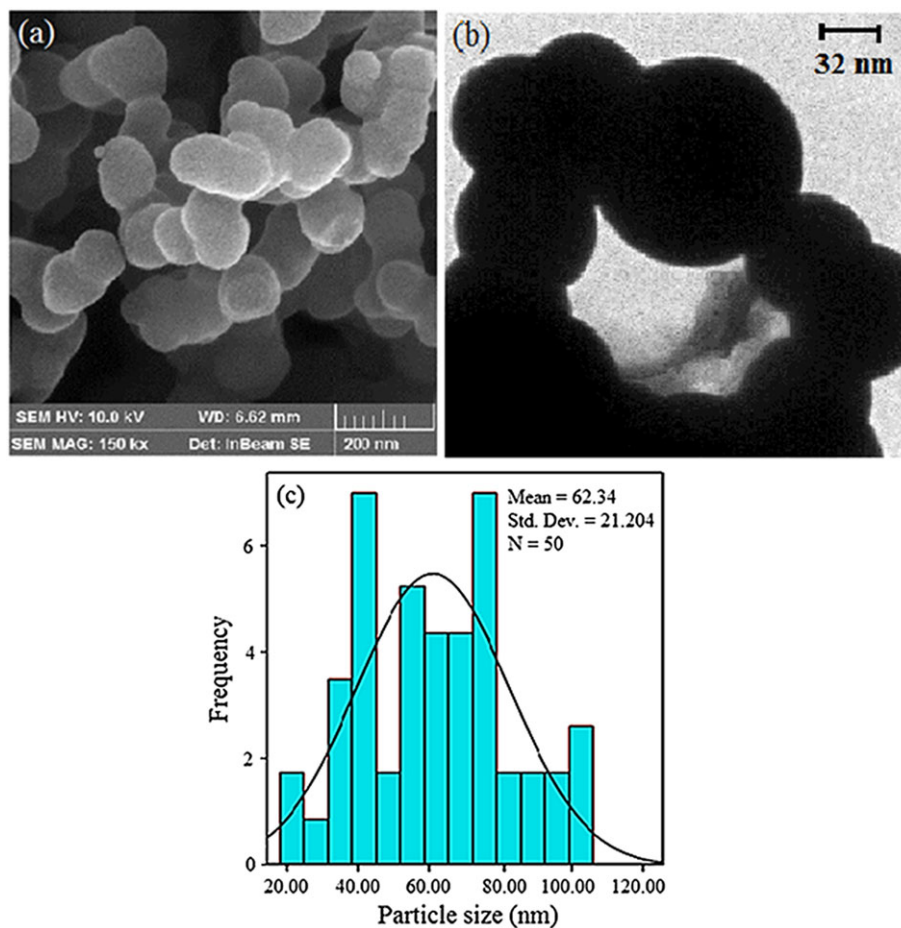


FIGURE 9 SEM photograph of nanocatalyst (a), TEM image of nanocatalyst (b) The histogram of the particle size distribution (c)

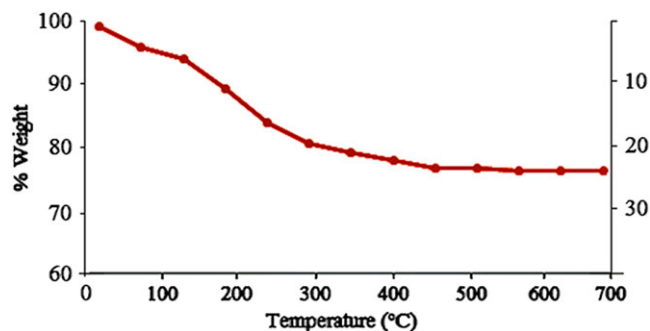


FIGURE 10 TGA curve of catalyst

of water molecules. The second weight loss (16%) in the range of 140 to 440 °C is attributed to the condensation of P-OH groups. After this temperature, no weight loss was observed at 700 °C.^[60]

3.4 | Catalytic activity

After preparation and characterization of the catalyst, the catalytic activity was tested in MBH reaction, using methyl acrylate and 4-methoxybenzaldehyde as the model substrates by changing the reaction parameters such as the amount of catalyst, reaction temperature, the molar ratio of reactants, type of aldehyde and solvent.

3.4.1 | The effect of catalyst amount

The reaction was carried out under the following conditions in the presence of 5–50 mg of catalyst:

room temperature, reaction time 12 hr and methyl acrylate/4-methoxybenzaldehyde mole ratio 1:1.

The results of the % conversion of methyl acrylate/4-methoxybenzaldehyde to the reaction product are shown in Table 1. By increasing the mass of catalyst from 5 to 20 mg, the conversion of two substances increases from 45 to 96%, which is due to the increase in the number of catalyst active sites but the mass of more than 20 mg reduces the reaction efficiency. The proposed mechanism is presented in Scheme 5. Step 1 involves a Michael-type addition of the catalyst from nitrogen (*) to the *beta*-carbon of the alkene.^[57,58] The resulting zwitterionic compound (A) is formed. In step 2 (as the rate-determining step (RDS)), by the nucleophilic attack of (A) on the aldehyde, intermediate B is formed. Finally, the product C is produced by transferring, removing hydrogen, and exiting the catalyst.

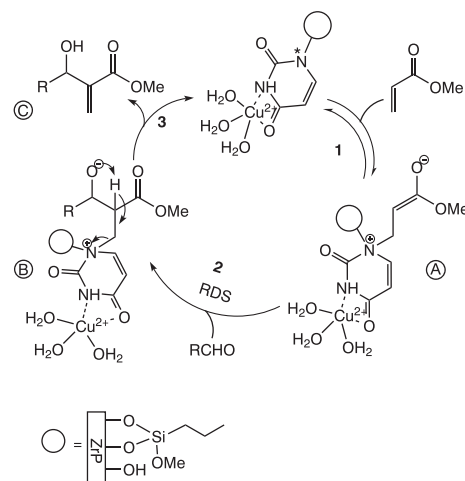
It is guessed that increasing the catalyst content by more than 20 mg can prevent the effective interactions between substance molecules in step 2. For this reason, the percentage of conversion is reduced. As noted in Section 1, a metal can accelerate the catalysis of the MBH reactions.^[13] The interaction of carbonyl groups in

TABLE 1 The effect of catalyst amount for the reaction of methyl acrylate with 4-methoxybenzaldehyde^a

Entry	The catalyst amount (mg)	The % conversion of methyl acrylate/4-methoxybenzaldehyde ^b
1	5	45
2	7	47
3	10	60
4	12	71
5	15	80
6	17	89
7	20	96
8	22	78

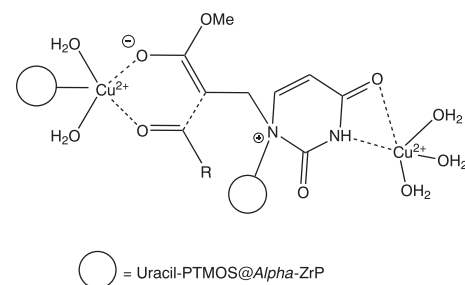
^aReaction conditions: methyl acrylate (1.2 mmol), 4-methoxybenzaldehyde (1.0 mmol), r. t., time (12 hr) and DMF (3.0 ml).

^bisolated yield.



SCHEME 5 The proposed mechanism for MBH reaction

methyl acrylate and aldehyde with copper as a catalyst metal section leads to the activation of the carbonyl groups (Scheme 6).^[13,61] As a result, the Michael-type addition in step 1 and the nucleophilic attack in step 2 are better done.



SCHEME 6 Metal can accelerate the catalysis of the MBH reactions

3.4.2 | The effect of reaction temperature and solvent

The MBH reaction of methyl acrylate/4-methoxybenzaldehyde was carried out from room temperature (25 °C) to 40 °C. As is clear from results, the increase in temperature did not affect the reaction efficiency. So the ambient temperature was chosen as the optimum temperature for the reaction (Table 2, Entry 1).

The solvent effect for the MBH reaction was also surveyed. The best result was obtained in the presence of DMF as solvent (Table 2, Entry 1).

3.4.3 | The effect of molar ratio of reactants and type of aldehyde

Several tests were performed to establish the effect of reactant ratio on % conversion by changing the mole ratio of the methyl acrylate/4-methoxybenzaldehyde from 1:2 to 2:1, in the same conditions (Table 3). It was observed that when the mole ratio of methyl acrylate/4-methoxybenzaldehyde was changed from 1:1 to 1.2:1, the percentage of conversion increased (From 85% to 96%). The change in the mole ratio of 4-methoxybenzaldehyde/methyl acrylate from 1:1 to 2:1 did not affect the conversion. Thus, the optimum mole ratio was found to be 1.2:1 for methyl acrylate/4-methoxybenzaldehyde (Table 3, Entry 2). According to the proposed mechanism in 'The effect of catalyst amount' section, with an increase in the concentration of methyl acrylate, the contact surface of this material with the catalyst active sites as the starting point of the MBH reaction increases. Therefore, better conditions for the absorption of aldehyde molecules are provided. But increasing the mole ratio of tow materials to more than 1.2:1, increases the steric hindrance around

TABLE 2 The effect of temperature and solvent for the reaction of methyl acrylate with 4-methoxybenzaldehyde^a

Entry	T (°C)	solvent	Yield ^b
1	25	DMF	96
2	30	DMF	95
3	35	DMF	95
4	40	DMF	96
5	25	DMSO	92
6	25	CH ₃ CN	80
7	25	THF	86
8	25	EtOH	75

^aReaction conditions: methyl acrylate (1.2 mmol), 4-methoxybenzaldehyde (1.0 mmol), time (12 hr), amount of catalyst (20 mg) and DMF (3.0 ml).

^bisolated yield.

TABLE 3 The effect of molar ratio of reactants for the reaction of methyl acrylate with 4-methoxybenzaldehyde^a

Entry	The mole ratio of methyl acrylate/4-methoxybenzaldehyde	Yield ^b
1	1:1	85
2	1.2:1	96
3	1.4:1	91
4	1.6:1	80
5	1.8:1	76
6	1.2:1.1	95
7	1.2: 1.3	90

^aReaction conditions: time (12 hr), amount of catalyst (20 mg), r. t. and DMF (3.0 ml).

^bisolated yield.

the catalyst surface. Therefore, aldehyde molecules cannot approach the catalytic effective surface (Table 3, Entry 4–7). This problem reduces the conversion of raw materials to the reaction product.

Finally, the effect of the selected aldehydes on the reaction efficiency has been studied (Table 4). The results showed that the MBH reaction in the presence of an activated vinyl system with aldehydes carrying electron-withdrawing substituents has a higher efficiency

TABLE 4 The MBH reaction of various aldehyde with methyl acrylate^a

Entry	Aldehyde	Time (h)	Yield (%) ^b
1	Benzaldehyde	12	76
2	3-Nitrobenzaldehyde	10	95
3	3-Methoxybenzaldehyde	12	90
4	Methyl 4-formylbenzoate	10	95
5	3-Pyridinecarboxaldehyde	8.5	100
6	4-Bromobenzaldehyde	12	92
7	4-Methoxybenzaldehyde	12	87
8	2-Naphthaldehyde	10	98
9	4-Chlorobenzaldehyde	12	93
10	2-Bromobenzaldehyde	11	90
11	Salicylaldehyde	11	92
12	5-Bromosalicylaldehyde	11	90

^aReaction conditions: aldehyde (1.0 mmol), methyl acrylate (1.2 mmol), DMF (3 ml), catalyst (20 mg), r. t.,

^bisolated yield.

and shorter time than other aldehydes carrying electron-releasing substituents. Compared with other aldehydes, 3-pyridinecarboxaldehyde acts as a very active substance and the reaction is performed in its presence with excellent efficiency and low time (Table 4, Entry 5).

In Table 5, instead of methyl acrylate, 2-cyclopentenone and acrylamide were used as acceptor. The results of the aldehyde type in section 'The effect of molar ratio of reactants and type of aldehyde' are also observed in this section. In addition, methyl acrylate is more effective than the other active vinyl systems used in this MBH reaction.

3.4.4 | Recyclability characteristic of catalyst

The ability to recycle the catalyst determines its sustainability. The regenerated catalyst and its recycling characteristic have been studied. This is represented in Figure 11. In order to investigate this property, the MBH reaction between methyl acrylate and 4-methoxybenzaldehyde was performed in the presence of α -ZrP/Uracil/ Cu^{2+} as the model reaction under the optimum conditions. At the end of the reaction, the catalyst was separated by centrifugation and washed

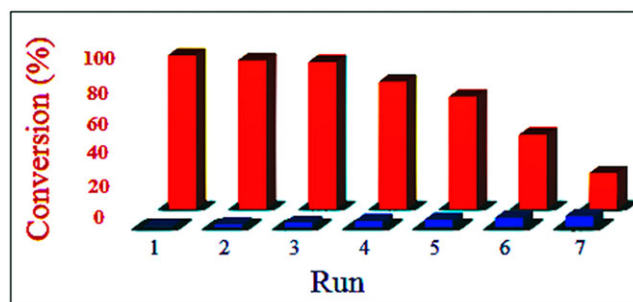


FIGURE 11 Recyclability of the catalyst

thoroughly with ethyl acetate. The catalyst was dried at 50 °C and reused for the next run. The recycling test showed that the catalyst was used up to 5 times without significantly reducing the reaction efficiency. The catalyst activity and the conversion of reactants to the product were reduced after the 5th runs. This observation was supported by XRD and TEM analysis of the recycled catalyst. The XRD patterns of the new and recovered catalyst are similar but the peaks are broadened in the XRD pattern of the recovered catalyst after being subjected to 5 runs (Figure 12).

As shown in Figure 13, the TEM images of the recycled catalyst and the fresh catalyst are very similar

TABLE 5 The MBH reaction of various aldehyde with activated vinyl^a

Entry	Aldehyde	activated vinyl	Time (h)	Yield (%) ^b
1	Benzaldehyde	2-cyclopentenone	15	74
2	3-Nitrobenzaldehyde	2-cyclopentenone	13	90
3	4-Methoxybenzaldehyde	2-cyclopentenone	15	83
4	2-Naphthaldehyde	2-cyclopentenone	15	90
5	3-Pyridinecarboxaldehyde	2-cyclopentenone	12	92
6	Benzaldehyde	acrylamide	15	70
7	3-Nitrobenzaldehyde	acrylamide	13	80
8	4-Methoxybenzaldehyde	acrylamide	15	77
9	2-Naphthaldehyde	acrylamide	13	85
10	3-Pyridinecarboxaldehyde	acrylamide	12	85

^aReaction conditions: aldehyde (1.0 mmol), activated vinyl (1.2 mmol), DMF (3 ml), catalyst (20 mg), r. t.,

^bisolated yield.

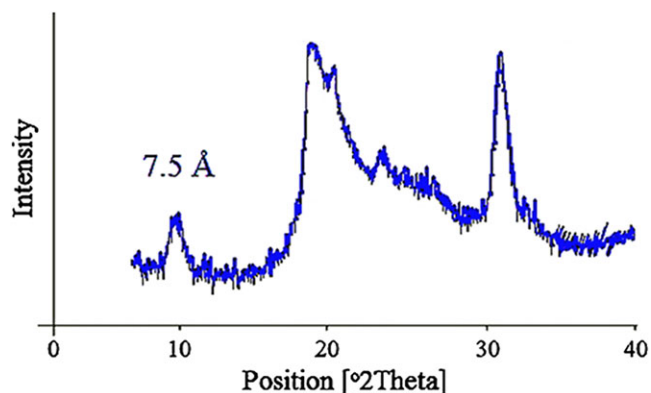


FIGURE 12 XRD pattern of catalyst after 5th runs

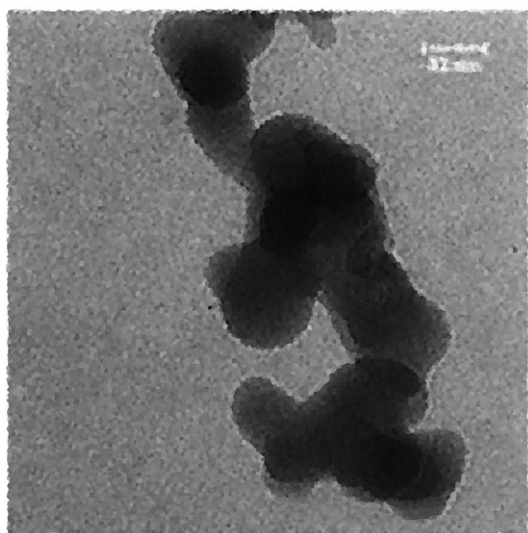


FIGURE 13 TEM image of catalyst after 5th runs

and there is no noteworthy change in the recovered catalyst structure. In order to prove this point that the prepared catalyst is heterogeneous, a hot filtration test was conducted during the reaction of methyl acrylate and 4-methoxybenzaldehyde. So that the heterogeneous catalyst was separated from the hot reaction mixture by filtration after 6 hr. The remaining solution was then allowed to react for another 6 hr. The results showed that in these conditions, the reactants have not been converted. In addition, the ICP result from the resultant supernatant showed that only 0.05 ppm of copper species was lost into solution during the reaction. These observations are evidence of high catalyst activity and the catalytic system stability.

The results of the nitrogen adsorption–desorption analysis of catalyst after 5th runs indicate that the nanoparticles of the catalyst do not clump during the reaction and maintain their high specific surface area (110.7 m² g⁻¹).

3.4.5 | The importance of α -ZrP in the role of α -ZrP/Uracil/Cu²⁺ as a catalyst in MBH reaction

For this purpose, Non-supported 1-methyluracil/Cu (II) catalyst was prepared. This way, 1-methyluracil was purchased from Sigma-Aldrich. The synthesis of 1-methyluracil/Cu (II) was performed according to the reported methodology.^[62] After preparation of 1-methyluracil/Cu (II), this combination as the catalyst was tested in MBH reaction, using methyl acrylate and 4-Methoxybenzaldehyde as the model reaction. After 48 hr, the reaction was carried out to 70% efficiency. In the meantime, catalyst separation was very difficult and its ability to recover and reuse was zero. The MBH reaction with 4-Methoxybenzaldehyde and 2-cyclopentenone was also carried out in the presence of 1-methyluracil/Cu (II) as the catalyst. After 48 hr, the reaction was carried out to 55% efficiency. The presence of α -ZrP as a nanosupport plays a very important role in the α -ZrP/Uracil/Cu²⁺ function as a catalyst in the Morita-Baylis-Hillman reaction.

4 | CONCLUSIONS

Briefly, we have reported the preparation of a new and efficient heterogeneous catalyst based on α -zirconium phosphate (α -ZrP) nanoparticles for the Baylis-Hillman reaction. α -ZrP serves as a sustainable support for (3-iodopropyl) trimethoxysilane as a linker, uracil as a ligand and Cu (II) as a metal section in the catalyst structure. The linker and ligand do not intercalate into the layers of the α -ZrP support. These factors, in addition to increasing the reaction efficiency, significantly reduce the reaction time. The prepared catalyst can be easily recycled and this catalytic system offers negligible leaching of Cu (II) to the reaction media and high catalytic activity over five successive runs. In general, this research is the first report of applying the {uracil-Cu}-propyltrimethoxysilane immobilized on α -ZrP nanoparticles as an effective catalyst in the Morita-Baylis-Hillman Reaction.

ACKNOWLEDGMENTS

The authors are thankful to research Council of Isfahan University of Technology (IUT), and Isfahan Science and Technology Town (ISTT) for their supports.

ORCID

Abdol R. Hajipour  <http://orcid.org/0000-0002-7737-0558>

REFERENCES

- [1] K. I. Morita, Z. Suzuki, H. Hirose, *Bull. Chem. Soc. Jpn.* **1968**, *41*, 2815.
- [2] D. Basavaiah, G. Veeraraghavaiah, *Chem. Soc. Rev.* **2012**, *41*, 68.
- [3] D. Basavaiah, B. S. Reddy, S. S. Badsara, *Chem. Rev.* **2010**, *110*, 5447.
- [4] M. L. Bode, P. T. Kaye, *Tetrahedron Lett.* **1991**, *32*, 5611.
- [5] D. Basavaiah, A. J. Rao, T. Satyanarayana, *Chem. Rev.* **2003**, *103*, 811.
- [6] S. E. Drewes, G. H. Roos, *Tetrahedron* **1988**, *44*, 4653.
- [7] S. Bhowmik, S. Batra, *Curr. Org. Chem.* **2014**, *18*, 3078.
- [8] C. G. Lima-Junior, M. L. Vasconcellos, *Bioorganic Med. Chem.* **2012**, *20*, 3954.
- [9] A. Patra, S. Batra, A. P. Bhaduri, A. Khanna, R. Chander, M. Dikshit, *Bioorganic Med. Chem.* **2003**, *11*, 2269.
- [10] S. E. Drewes, O. L. Njamela, N. D. Emslie, N. Ramesar, J. S. Field, *Synth. Commun.* **1993**, *23*, 2807.
- [11] T. Kataoka, H. Kinoshita, S. Kinoshita, T. Iwamura, S. I. Watanabe, *Angew. Chem. Int. Ed.* **2000**, *112*, 2448.
- [12] Y. Liu, **2011**, PhD Thesis. Imu.
- [13] V. K. Aggarwal, G. J. Tarver, R. McCague, *Chem. Comm.* **1996**, *24*, 2713.
- [14] E. Ciganek, *Org. React.* **1997**.
- [15] V. K. Aggarwal, A. Mereu, G. J. Tarver, R. McCague, *J. Org. Chem.* **1998**, *63*, 7183.
- [16] M. Kawamura, S. Kobayashi, *Tetrahedron Lett.* **1999**, *40*, 1539.
- [17] Y. Sohtome, A. Tanatani, Y. Hashimoto, K. Nagasawa, *Tetrahedron Lett.* **2004**, *45*, 5589.
- [18] N. T. McDougal, S. E. Schaus, *J. Am. Chem. Soc.* **2003**, *125*, 12094.
- [19] A. Clearfield, G. D. Smith, *Inorg. Chem.* **1969**, *8*, 431.
- [20] R. Silbernagel, A. Diaz, E. Steffensmeier, A. Clearfield, J. Blumel, *J. Mol. Catal. Chem.* **2014**, *394*, 217.
- [21] L. Sun, W. J. Boo, R. L. Browning, H. J. Sue, A. Clearfield, *Chem. Mater.* **2005**, *17*, 5606.
- [22] N. Carlsson, H. Gustafsson, C. Thorn, L. Olsson, K. Holmberg, B. Akerman, *Adv. Colloid Interface Sci.* **2014**, *205*, 339.
- [23] F. Bellezza, A. Cipiciani, U. Costantino, F. Fringuelli, M. Orru, O. Piermatti, F. Pizzo, *Catal. Today* **2010**, *152*, 61.
- [24] J. Guenther, J. Reibenspies, J. Blumel, *Synthesis, Adv. Synth. Catal.* **2011**, *353*, 443.
- [25] J. Tuteja, H. Choudhary, S. Nishimura, K. Ebitani, *Chem. Sus. Chem.* **2014**, *7*, 96.
- [26] A. R. Hajipour, H. Karimi, *Appl. Catal., A* **2014**, *482*, 99.
- [27] A. Diaz, M. L. Gonzalez, R. Perez, J. David, A. Mukherjee, A. Baez, J. L. Colon, *Nanoscale* **2013**, *5*, 11456.
- [28] A. Diaz, A. David, R. Perez, M. L. Gonzalez, A. Baez, S. E. Wark, J. L. Colon, *Biomacromolecules* **2010**, *11*, 2465.
- [29] A. Sinhamahapatra, N. Sutradhar, B. Roy, A. Tarafdar, H. C. Bajaj, A. B. Panda, *Appl. Catal., A* **2010**, *385*, 22.
- [30] F. Zhang, Y. Xie, W. Lu, X. Wang, S. Xu, X. Lei, *J. Colloid Interface Sci.* **2010**, *349*, 571.
- [31] A. R. Hajipour, H. Karimi, *Mater. Lett.* **2014**, *116*, 356.
- [32] A. Diaz, V. Saxena, J. Gonzalez, A. David, B. Casanas, C. Carpenter, M. D. Hussain, *Chem. Comm.* **2012**, *47*, 1754.
- [33] V. K. Gupta, D. Pathania, P. Singh, B. S. Rathore, P. Chauhan, *Carbohydr. Polym.* **2013**, *95*, 434.
- [34] Y. Yang, C. Liu, P. R. Chang, Y. Chen, D. P. Anderson, M. Stumborg, *J. Appl. Polym. Sci.* **2010**, *115*, 1089.
- [35] Z. Wang, D. Tao, G. Guo, S. Jin, F. Wei, W. Qian, J. Guo, *Mater. Lett.* **2006**, *60*, 3104.
- [36] M. Aleahmad, H. G. Taleghani, H. Eisazadeh, *Synth. Met.* **2011**, *161*, 990.
- [37] S. Wei, M. Lizu, X. Zhang, J. Sampathi, L. Sun, M. F. Milner, *High Perform. Polym.* **2013**, *25*, 25.
- [38] H. Lu, C. A. Wilkie, M. Ding, L. Song, *Polym. Degrad. Stab.* **2011**, *96*, 1219.
- [39] M. Casciola, D. Capitani, A. Donnadio, G. Munari, M. Pica, *Inorg. Chem.* **2010**, *49*, 3329.
- [40] B. M. Mosby, A. Diaz, V. Bakhmutov, A. Clearfield, *Inorg. Chem.* **2013**, *23*, 7680.
- [41] H. Nakayama, *Phosphorus, R. B.* **2009**, *23*, 1.
- [42] K. I. Segawa, Y. Kurusu, Y. Nakajima, M. Kinoshita, *J. Catal.* **1985**, *94*, 491.
- [43] G. A. Mekhemer, *Colloids Surf., A* **1998**, *141*, 227.
- [44] A. Jain, A. M. Shore, S. C. Jonnalagadda, K. V. Ramanujachary, A. Mugweru, *Appl. Catal., A* **2015**, *489*, 72.
- [45] D. Fildes, V. Caignaert, D. Villemin, P. A. Jaffres, *Green Chem.* **2001**, *52*.
- [46] M. Pica, *Catalysts* **2017**, *7*, 190.
- [47] M. Turco, P. Ciambelli, G. Bagnasco, A. La Ginestra, P. Galli, C. Ferragina, *J. Catal.* **1989**, *117*, 355.
- [48] H. Karimi, *IJSTS. Transactions A: Science* **2016**, *1*.
- [49] C. Merckle, S. Haubrich, J. Blumel, *J. Organomet. Chem.* **2001**, *627*, 44.
- [50] S. Reinhard, K. D. Behringer, J. Blumel, *New J. Chem.* **2003**, *27*, 776.
- [51] A. R. Hajipour, P. Abolfathi, *New J. Chem.* **2017**, *41*, 2386.
- [52] R. M. Bota, K. Houthoofd, P. J. Grobet, P. A. Jacobs, *Catal. Today* **2010**, *152*, 99.
- [53] J. Goscianska, M. Ziolek, E. Gibson, M. Daturi, *Catal. Today* **2010**, *152*, 33.
- [54] L. Sun, W. J. Boo, H. J. Sue, A. Clearfield, *New J. Chem.* **2007**, *31*, 39.
- [55] A. R. Hajipour, H. Karimi, A. Koohi, *Chin. J. Catal.* **2015**, *36*, 1109.
- [56] V. Pale, Z. Giedraityte, X. Chen, O. Lopez-Acevedo, I. Tittonen, M. Karppinen, *Sci. Rep.* **2017**, *7*, 6982.
- [57] M. A. Kurinovich, J. K. Lee, *J. Am. Chem. Soc.* **2000**, *122*, 6258.
- [58] M. A. Kurinovich, J. K. Lee, *J. Am. Soc. Mass Spectrom.* **2002**, *12*, 985.
- [59] A. Khalafi-Nezhad, A. Zare, A. Parhami, M. S. Rad, *ARKIVOC* **2006**, *12*, 161.
- [60] M. Kamaruzama, S. Chin, *J. Appl. Sci.* **2014**, *14*, 1339.

- [61] D. J. V. van Steenis, T. Marcelli, M. Lutz, A. L. Spek, J. H. van Maarseveen, H. Hiemstra, *Adv. Synth. Catal.* **2007**, *394*, 281.
- [62] Y. P. Patil, M. Nethaji, *J. Mol. Struct.* **2015**, *1081*, 14.

SUPPORTING INFORMATION

Additional supporting information may be found online in the Supporting Information section at the end of the article.

How to cite this article: Hajipour AR, Zakery S. α -ZrP/Uracil/Cu²⁺ nanoparticles as an efficient catalyst in the Morita-Baylis-Hillman reaction. *Appl Organometal Chem.* 2018;e4487. <https://doi.org/10.1002/aoc.4487>